POLİTEKNİK DERGİSİ

JOURNAL of POLYTECHNIC

ISSN: 1302-0900 (PRINT), ISSN: 2147-9429 (ONLINE)
URL: http://dergipark.org.tr/politeknik

Numerical investigation of radius dependent solidity effect on H-type vertical axis wind turbines

Yarıçapa bağlı katılık oranının bir H-tip dikey eksenli rüzgâr türbinine etkisinin sayısal olarak incelenmesi

***Yazar(lar) (Author(s))**: Ahmet Fatih KAYA[1], Himmet Erdi TANÜRÜN[2], Adem ACIR[3]*

ORCID[1]: 0000-0002-7888-0250

ORCID[2]: 0000-0001-7814-7043

ORCID[3]: 0000-0002-9856-3623

Bu makaleye şu şekilde atıfta bulunabilirsiniz(To cite to this article): Kaya A.F., Tanürün H.E. and Acır A., "Numerical investigation of radius dependent solidity effect on H-type vertical axis wind turbines", ***Politeknik Dergisi***, 25(3): 1007-1019, (2022).

Erişim linki (To link to this article): http://dergipark.org.tr/politeknik/archive

DOI: **10.2339/politeknik.799767**

Numerical Investigation of Radius Dependent Solidity Effect on H-Type Vertical Axis Wind Turbines

Highlights

- *Effect of radius dependent solidity to the aerodynamic performance of a h-rotor Darrieus wind turbine was investigated.*
- *2-D numerical analyses were performed by using realizable k-epsilon turbulence model.*
- *Turbulence Kinetic Energy and Pressure Contours around the blades were examined.*

Graphical Abstract

Solidity value changes with rotor radius, chord length and number of blades. In this study, only rotor radius was changed. By using Ansys – Fluent software, two Dimensional CFD (Computational Fluid Dynamics) analyses were performed to investigate the solidity effect to the aerodynamic performance of a h-rotor wind turbine.

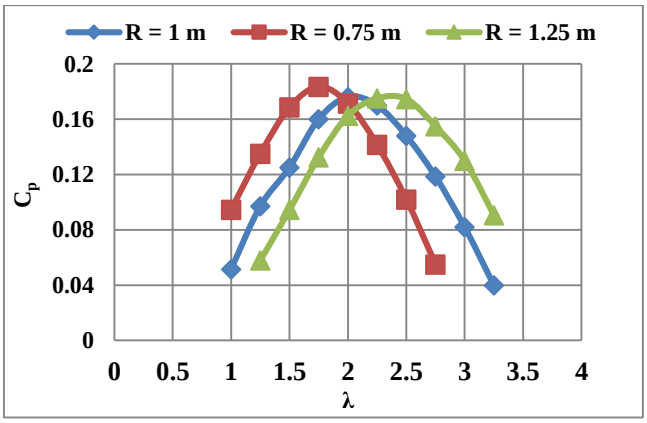

Figure. Power coefficient versus TSR as a function of Solidity

Aim

The aim of this research examine the solidity effect to a h-darrieus wind turbine and improve the aerodynamic performance.

Design & Methodology

Three different wind turbine models were created with Catia v5 software. Two Dimensional numerical analyses were performed with using realizable k-epsilon turbulence model by using Ansys – Fluent. An experimental study was validated after reaching mesh independence. Pressure and turbulent kinetic energy contours around blades were analysed.

Originality

Vertical Axis Wind Turbines are usually operated in small areas. They are cheap and easy to build, but their efficiency is lower than Horizontal Axis Wind Turbines. Their aerodynamic characteristics need to be improved.

Findings

An observed maximum power coefficient was increased by 4.25% with decreasing rotor radius. Also, it was declined by 0.57% with increasing rotor radius.

Conclusion

The wind turbine with a higher solidity has a more coefficient of power in lower Tsr values. With the decrease of solidity, more coefficient of power can be observed in higher Tsr values. An appropriate rotor radius can be found for different tsr values on created Cp – Tsr chart.

Declaration of Ethical Standards

The author(s) of this article declare that the materials and methods used in this study do not require ethical committee permission and/or legal-special permission.

Numerical Investigation of Radius Dependent Solidity Effect on H-Type Vertical Axis Wind Turbines

Araştırma Makalesi / Research Article

Ahmet Fatih KAYA[1*], Himmet Erdi TANÜRÜN[2], Adem ACIR[2]

[1]Fen Bilimleri Enstitüsü, Enerji Sistemleri Mühendisliği Anabilim Dalı, Gazi Üniversitesi, Türkiye
[2]Teknoloji Fakültesi, Enerji Sistemleri Mühendisliği Bölümü, Gazi Üniversitesi, Türkiye

(Geliş/Received : 24.09.2020 ; Kabul/Accepted : 22.11.2020 ; Erken Görünüm/Early View : 03.12.2020)

ABSTRACT

In this study, radius-dependent solidity effect to the aerodynamic characteristic of a three bladed H-rotor Darrieus wind turbine consisting of NACA 0021 profile blades was investigated numerically in Ansys Fluent 14.1 software. After achieving independence from the mesh, the numerical method was validated with the experimental data and then numerical analyses were performed for different solidity values. Results show that the higher efficiency can be obtained both in low Type Speed Ratio (TSR) values with the increase of solidity and in high TSR values with the decrease in solidity. Power coefficient (Cp) has been enhanced as 4.25% with 0.75 m (M1) and Cp has been reduced as 0.57% with 1.25 m (M3) rotor radius according to 1 m rotor radius (M2), respectively.

Keywords: Numerical analysis, darrieus wind turbine, H-rotor, tip speed ratio, solidity.

Yarıçapa Bağlı Katılık Oranının bir H-Tip Dikey Eksenli Rüzgâr Türbinine Etkisinin Sayısal Olarak İncelenmesi

ÖZ

Bu çalışmada yarıçapa bağlı olarak değiştirilen katılık oranının, NACA 0021 kanat profiline sahip 3 kanatlı H-tip dikey eksenli rüzgar türbini aerodinamik performansına olan etkisi sayısal olarak Ansys – Fluent 14.1 yazılımında incelenmiştir. Meshten bağımsızlığa ulaşıldıktan sonra kullanılan sayısal methodlar deneysel çalışmadan elde edilen sonuçlar ile doğrulanmış ve farklı katılık oranlarında sayısal analizler tekrarlanmıştır. Sonuçlar incelendiğinde, katılık oranının artması ile birlikte düşük kanat uç hız oranlarında (TSR), katılık oranının azalması ile birlikte ise yüksek TSR değerlerinde daha yüksek aerodinamik verim elde edileceği görülmüştür. Gözlemlenen en büyük güç katsayıları, 1 m yarıçapa sahip olan turbine göre (Cp) 0.75 m yarıçapa sahip olan (M1) türbinde %4.25 artmış, 1.25 m yarıçapa sahip olan (M3) türbinde ise % 0.57 azalmıştır.

Anahtar Kelimeler: Sayısal analiz, darrieus rüzgar türbini, H-rotor, kanat uç-hız oranı, katılık.

1. INTRODUCTION

Concerns about global problems such as environmental pollution and global warming because of using fossil fuels have been increasing in recent years. Using renewable energy sources contributes to reduction of the negative effects of traditional fuels on the environment and human health, as well as on the sustainable development of societies. Wind turbines can meet the energy demand that will increase gradually in the near future with other energy resources. They convert kinetic energy to the mechanical energy. Generator produces electricity with this mechanical energy. There are 2 different wind turbine types according to their rotation axes, vertical axis wind turbines (VAWT) and horizontal axis wind turbines (HAWT) [1]. VAWT's have some advantages over HAWT, they can catch wind in any direction, vertical rotor shaft and heavy loads like generators can be placed on the ground [2].

VAWT's are classified into two types according to their working principle. The drag type model which is called savonious wind turbine rotating with the aerodynamic forces acting the blades and the lift type model which is called Darrieus wind turbine, pressure differences on the lower and upper blade surfaces rotate wind turbine [3].

For the last few years, a large amount of research has been done about wind turbines. In these studies, effect of some geometric and operational parameters such as number of blades [4-8], blade pitch angle [9-11], Reynolds number [12-15], turbulence properties [16-19], blade profile [20-22] and solidity [23,24] on aerodynamic performance of Darrieus wind turbines were examined numerically or experimentally and optimization studies were carried out to get maximum power from wind turbines.

*Sorumlu Yazar (Corresponding Author)
e-posta : ahmetfatih.kaya@gazi.edu.tr

Li et al. experimentally investigated the blade number effect and pitch angle on wind turbine aerodynamic performance in a H-Rotor wind turbine with of NACA 0021 blade profile. In their study, increased blade number resulted in obtained maximum Cp value get decreased. They stated that energy production will be higher by using a 2-bladed wind turbine in regions with high wind speeds and 5-blade wind turbine model in regions with low wind speeds. At the same time, they observed that the highest aerodynamic performance was attained by using blades which has 6° pitch angle on the wind turbine with 2 blades, 8° on the turbine with 3 and 4 blades and 12° on the wind turbine with 5 blades [4]. Yang et al. experimentally and numerically examined the pitch angle effect on a 2-bladed H-rotor darrieus wind turbines aerodynamic characteristic. At optimum TSR value, they observed that the highest aerodynamic performance with the turbine which has 6° blade pitch angle and they stated that the blade pitch angle has no effect to the aerodynamic performance so well as HAWTs. Also, they concluded that the pressure difference affecting blade surfaces reaches the maximum value when the azimuth angle was between 0-180° at 6° pitch angle and the azimuth angle was between 180-360° at 8° blade pitch angle [9]. Siddiqui et al. investigated numerically turbulence density effect to the offshore vertical axis wind turbines torque characteristic. They used realizable k-epsilon, standard k-epsilon and rng k-epsilon turbulence models. They reached the most reasonable results with using realizable k-e turbulence model. Their results indicate that the average torque value observed in the wind turbine decreased with the increase in turbulence density [16]. Zamani et al. performed a 3D CFD (Computational Fluid Dynamics) analyses with using SST k-ω turbulence model to investigate the J-shaped blade structure effect to the wind turbine torque and the power output. As a result, they observed that using the J-shape blade structure increased the wind turbine self-start capability, and also caused the rotor to be less affected by the dead-band region. In their study, they stated that the Cp value observed in the wind turbine increased by using J-shape blade structure in all TSR values except 1.8 [21]. Kumar and Baredar investigated solidity effects to the aerodynamic performance of small HAWT by changing number of blades. They concluded that with the increase of solidity, Cp values increased while rotor speed get decreased. Also, they observed that when the solidity decreased, observed Cp value decreased and rotor speed increased [23]. Alqurashi and Mohamed conducted a numerical analysis to investigate the blade profile effect to the wind turbine aerodynamic performance. They performed their analyses with using realizable k-epsilon turbulence model. As a result, the wind turbine with LS413 blade profile showed higher aerodynamic performance than other turbine models. At the same time, more tangential force and axial force coefficient were observed on the S1046 blade profile compared to the other 2 blade profiles, and they stated that the turbine model with S1046 blade profile has lower self-start capability than other turbine models [28].

In this study, two-dimensional (2D) CFD study was carried out using Ansys Fluent 14.1 software in order to investigate solidity effect to the Cp value observed in H-rotor Darrieus turbine. The three-bladed wind turbine which has 8° blade pitch angle with NACA 0021 airfoil was modelled using CATIA V5. The wind turbine aerodynamic performance for three different solidity values was analysed by changing the turbine rotor radius. The analyses were performed by showing turbulence kinetic energy, pressure and Cp values for different azimuth angles. As a result, obtained results in this study after reach mesh independence were compared with the experimental study.

2. FLOW FIELD SETUP

2.1. Basic Aerodynamics for H- Rotor Darrieus wind turbine

H- Darrieus wind turbines are a kind of vertical axis wind turbine. Usually, two or three blades are used. Cross arms connect the blades and rotating shaft. It was invented in 1931 by G.J.M Darrieus [25]. In Figure 1, a schematic presentation of a H-Darrieus wind turbine is given.

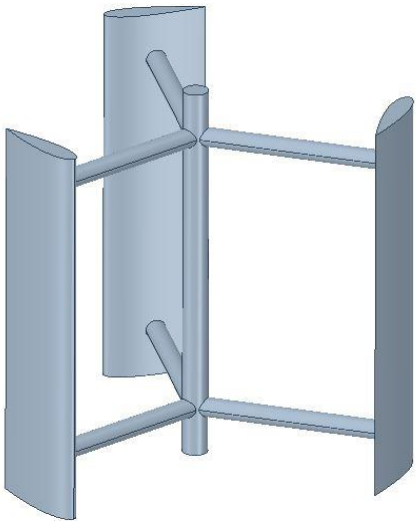

Figure 1. The schematic view of H-Darrieus wind turbine

Tip Speed Ratio expression is a reference dimensionless number used when determining the power coefficient and it is shown with the following equation;

$$\lambda = \mathrm{TSR} = \frac{\omega * R}{U} \quad (1)$$

In this equation, U indicates the wind speed, R is the turbine radius and ω shows the angular velocity. Turbine solidity (σ) strongly affects to the aerodynamic characteristic of a wind turbine. Solidity means the ratio of the area containing the material around the turbine rotor to the containing of air in that area [37].

$$\sigma = \frac{N*c}{2R} \quad (2)$$

N indicates the blade number, c indicates the length of the blades chord.

It is not possible to use all energy of the wind with using wind turbines. As seen in Eq. (3), Cp shows the wind turbine efficiency. The Cp value was determined as the highest 59% in analytical solutions which is defined as Betz number with the following equation;

$$C_p = \frac{P}{\frac{1}{2}\rho A U^3} \quad (3)$$

Here, P is the generated power from a wind turbine, ρ shows the density of air and A indicates the swept area of the turbine. In Eq. (4), swept area is in vertical wind turbines defined as;

$$A = D * H \quad (4)$$

Here, H and D represent the turbine height and the rotor diameter, respectively.

Moment coefficient (C_m) expression is shown in equation 5. In Eq. (6), the relation between the C_m and C_p is shown [26].

$$C_m = \frac{T}{\frac{1}{2}\rho A R U^2} \quad (5)$$

$$C_m = \frac{Cp}{\lambda} \quad (6)$$

The drag (F_D) and lift forces (F_L) occurring to the turbine blades vary depending on the turbine azimuth angle (θ). This forces can be determined as [27];

$$F_D = \frac{C_D \rho U^2 c}{2} \quad (7)$$

$$F_L = \frac{C_L \rho U^2 c}{2} \quad (8)$$

C_D is the drag coefficient and C_L is the lift coefficient.

Attack angle (α) is the angle between the wind direction towards the blades and its axis [28].

$$\alpha = \arctan\left[\frac{\sin\theta}{\lambda+\cos\theta}\right] \quad (9)$$

If the blade pitch angle (β) is taken into account;

$$\alpha = \arctan\left[\frac{\sin\theta}{\lambda+\cos\theta}\right] - \beta \quad (10)$$

Forces and velocity components affecting on H-rotor wind turbine were shown in Figure 2 [29].

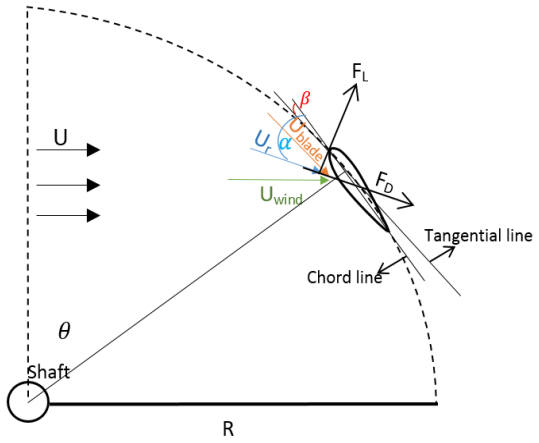

Figure 2. Velocities and forces acting one blade

2.2.Geometric and Operational Parameters

In this study, the geometric dimensions of the modelled turbine were kept the same as the geometric dimensions of the turbine which was used in the experimental study conducted by Li et al [4]. H-rotor wind turbine consisting NACA 0021 blade profile is modelled in two dimensions to be β = 8°. In Table 1, geometric parameters and operating conditions of the model used in this study are indicated.

Table 1. The Turbine Features

Parameter	Value	Parameter	Value
Airfoil	NACA 0021	Turbine Height, H	1,2 m
Number of Blades, N	3	Swept Area, A	2,4 m^2
Airfoil chord length, c	0,265 m	Wind Speed, U	8 m/s
Diameter, D	2 m	Turbulence Intensity	0,5 %

Figure 3 shows the structure of the four digit NACA 0021 blade profile used. First digit shows that the maximum curvature in percentage of the chord length is 0. Hence NACA 0021 airfoil has no camber, second digit is also equals to 0, which indicates the position of the camber. This means that the blade is symmetrical. Last two digits show the ratio of the chord length to the blade thickness.

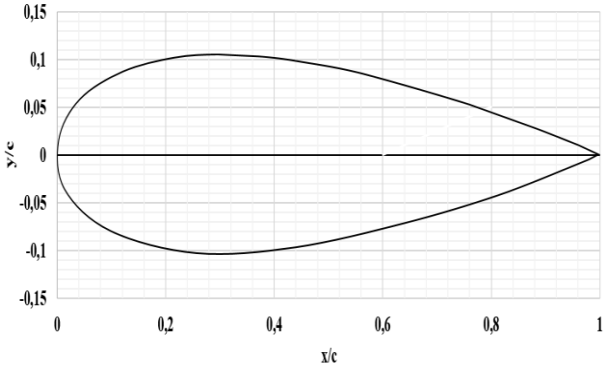

Figure 3. NACA 0021 Blade Profile

2.3.Computational Domain

It is extremely important to create a convenient flow field for numerical analysis in fluid mechanics problems. If the created region is too large, it increases the number of meshes, and thus the solution time is extended. As this region is smaller than it should be, it will cause the solution to get away from reality as it will cause inadequate flow modelling [30]. A separate zone (blade subdomain) has been created in the close surrounding of the turbine blades in order to increase mesh density. Interfaces have been defined to ensure the continuity of the flow and in order to ensure that there is no imbalance in the mesh dimensions between the blade subdomain - rotating domain and the rotating domain - stationary domain.

In a C-type flow area, the inlet boundary condition is 7R and the outlet boundary condition is 10R away from the turbine center. The symmetry boundary condition has been set for the top and bottom edges. In Figure 4, the flow area used during the analysis is shown.

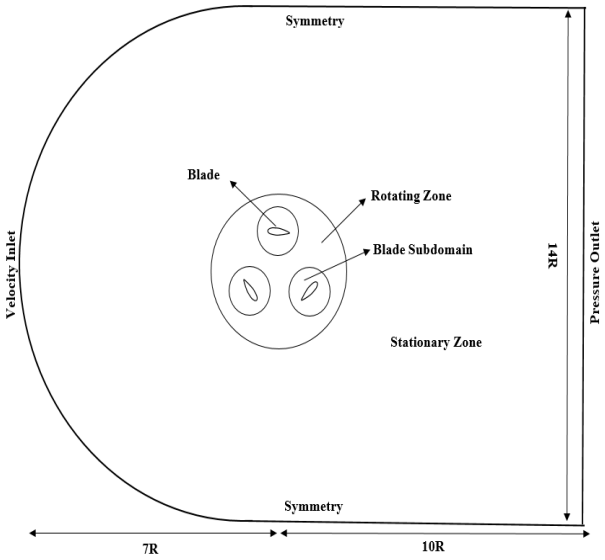

Figure 4. Computational Domain

2.4.Turbulence Model

The turbulence model used in the analysis is of great importance for the verification of the experimental study and the accuracy of the solution in the later stages. To solve the Unsteady Reynolds Averaged Navier - Stokes (URANS) equations, realizable k-epsilon turbulence model was used. There are many studies can be found in the literature using realizable k-epsilon turbulence model, which shows very close results to experimental data. [28,31-34].

The realizable k-epsilon turbulence model is generally recommended for flow analysis in rotating regions [31]. Transport equations used to calculate turbulence kinetic energy (k) and turbulence dissipation rate (ε) vary according to the standard k-epsilon turbulence model and the equations of this model are expressed as follows;

$$\frac{\partial}{\partial t}(\rho k)+\frac{\partial}{\partial x_j}(\rho k U_j)=\frac{\partial}{\partial x_j}\left[\left(\mu+\frac{\mu_t}{\sigma_k}\right)\frac{\partial k}{\partial x_j}\right]+G_m+G_n-\rho\varepsilon-Y_G+S_k \quad (11)$$

$$\frac{\partial}{\partial t}(\rho \varepsilon)+\frac{\partial}{\partial x_j}(\rho \varepsilon U_j)=\frac{\partial}{\partial x_j}\left[\left(\mu+\frac{\mu_t}{\sigma_\varepsilon}\right)\frac{\partial \varepsilon}{\partial x_j}\right]+\rho C_1 S\varepsilon-\rho C_2\frac{\varepsilon^2}{k+\sqrt{\upsilon\varepsilon}}+C_{1\varepsilon}\frac{\varepsilon}{k}C_{3\varepsilon}G_n+S_\varepsilon \quad (12)$$

$$C_1=\max\left[0.43,\frac{\eta}{\eta+5}\right],\ \eta=S\frac{k}{\varepsilon},\ S=\sqrt{2S_{ij}S_{ij}} \quad (13)$$

Here is G_m and G_n indicates production of turbulence kinetic energy because of the velocity gradients and buoyancy force, respectively. The expressions of σ_k and σ_ε indicate turbulence prandtl numbers. Y_G shows the contribution of dilatations in compressible turbulence to the dissipation rate, μ and μ_t *are* dynamic and turbulence viscosity, respectively. $C_{1\varepsilon}$ and $C_{3\varepsilon}$ values are constant, while S_ε and S_k are user dependent variables [32,35].

2.5. CFD Solver Setting

The solver settings to be used during CFD analysis are very important for the accuracy of the analyses. Between stationary and rotating zone, a sliding mesh was applied. The turbulence intensity was adjusted as 0.5% at inlet boundary condition. In order to solve the momentum, k and ε equations, the second order upwind formulation was used. Time step size (Δt) is determined at the time that the turbine takes each 1°. This is because, decreasing time step size too much causes solution will take longer time. Also, increasing time step size can result in unreasonable results.

While determining this time step size (Δt), the following path is followed;

For λ = 2, when U = 8 m / s and R = 0.1 m,

$$\omega = 16\,\frac{r}{s} \sim 916{,}7\,\frac{\text{degree}}{\text{sec.}} \quad (14)$$

A turbine rotating 916.7°/sec, approximately 1° angle,

$$\Delta t = \frac{1}{916{,}7} = 0{,}001091\frac{\text{sec.}}{\text{degree}} \text{ is complete} \quad (15)$$

Same operations were repeated for all other angular velocities. Number of time steps are set to provide the turbine for 12 revolutions. C_m value varies with λ value, on average it becomes constant between 5 and 12 revolutions.

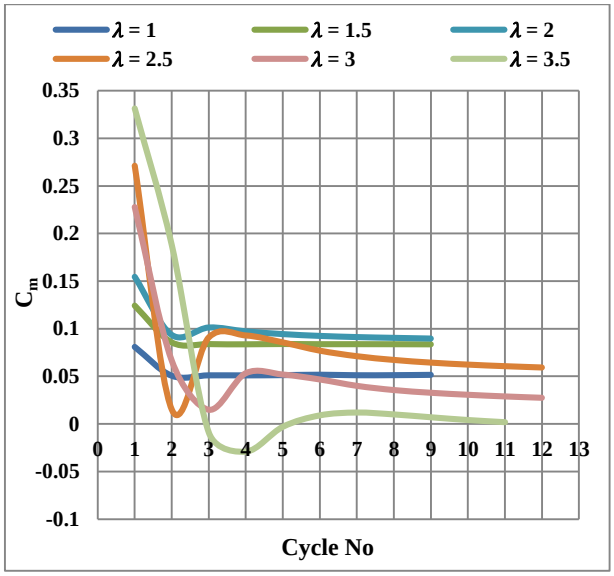

Figure 5. Averaged moment coefficient value varying with the number of cycles for Different λ values

Figure 5 shows in which range the Cm value stabilizes at different λ values. Due to the increase in the angular velocity of the model, it was seen that the turbine should take more turns to stabilize the value of C_m obtained from the turbine due to the concentration of vortex areas in the near part of the blades. The averaged C_m values were calculated by averaging the observed C_m values for each azimuthal angle in the last revolution of the turbine.

2.6. Mesh Independence

In numerical calculations, the solution time of the analysis is directly related to the number of meshes. Increased mesh number also results in longer solution time. If the number of meshes is less than it should be, the solution will be getting away from reality. Therefore, the most accurate results are obtained with the shortest time in analyses by using the most appropriate mesh number. Figure 6 shows the power coefficient values obtained in different mesh numbers. There is a fluctuation in the power coefficient value with the increasing elements number. Same trend can be observed in other studies [3, 21, 36].

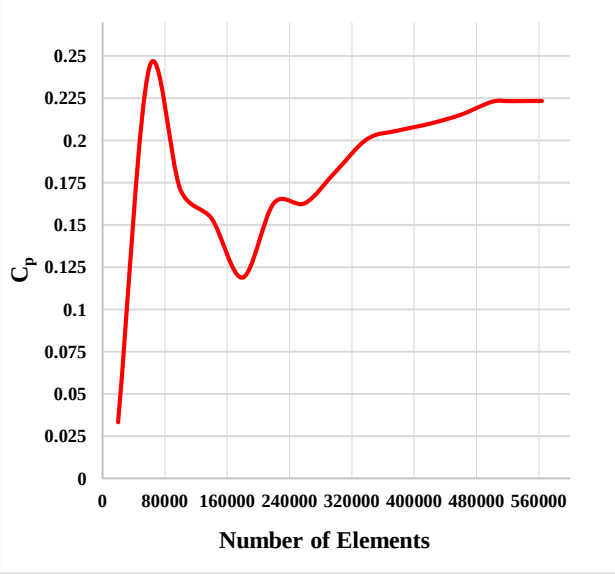

Figure 6. Mesh Independence

For λ = 2, according to numerical analyses with using realizable k-epsilon turbulence model made in 15 different mesh numbers in the range of 20583 and 564177 values, the difference between the power coefficient values calculated in 523611 and 564177 mesh numbers is less than 0.1%. According to this result, analyses were carried out in 523611 mesh number. While calculating this difference between C_p values, the following equation is used;

$$\%Dif. = \left|\frac{Cp\ (Mesh\ No\ 15) - Cp\ (Mesh\ No\ 14)}{Cp\ (Mesh\ No\ 15)}\right| * 100 \qquad (16)$$

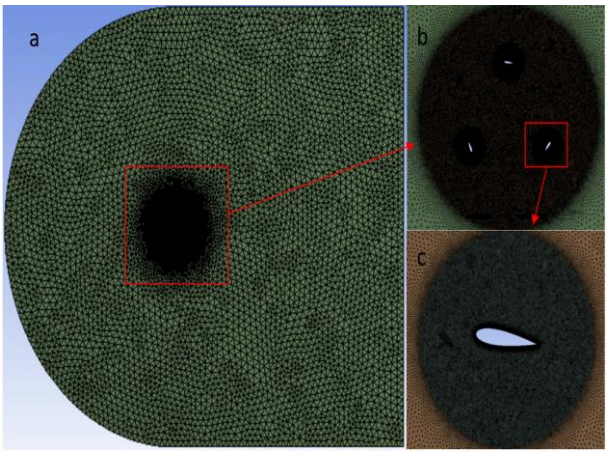

Figure 7. The mesh for VAWT (a) Computational domain (b) Inner Domain (c) Blade Subdomain

Figure 7 shows the mesh structure used for this study. When Figure 7 is examined, the number of meshes is intensified around the blades of the turbine by the method of inflation. The number of meshes from rotating zone to stationary zone has decreased gradually. This is because the flow characteristic around the blade structure changes rapidly, while the flow towards the enclosure endpoints is more stable.

3. RESULTS

In this study, the aerodynamic performance of 3-bladed H- rotor type VAWT with a height of 1.2 m was examined using Ansys Fluent 14.1 software in different solidity ratios. After achieving independence from the mesh, experimental study [4] was validated with this study. After that, the turbine radius was changed to be 0.75 m and 1.25 m, and the analyses were repeated at intervals of 0.25 TSR for each turbine radius.

3.1. Model Validation

The results obtained from experimental study and numerical analysis were shown in Fig. 8.

Investigations of the Figure, it is observed that the results obtained with the realizable k-epsilon turbulence model are very close to the experimental data, especially at low TSR values. At high TSR values, there is a difference between numerical and experimental results. This is because the rotor angular velocity reaches very large values at high TSR values, and dense vortex regions occur throughout and around spanwise. In 2D analyses, spanwise-vortex interaction is ignored while taking chord – vortex interactions into account [37]. This situation is not very important in the analysis since it is formed after the value of Cp in the λ - tsr chart. While the maximum Cp value was 0.189 in the experimental study which has been done by Li et al. [4], this value was 0.176 in this study. The margin of error is determined as 6.87%. This percentage is an acceptable value in the literature. The margin of error of the obtained results may be due to the difference in the dense vortex regions occur throughout and around spanwise.

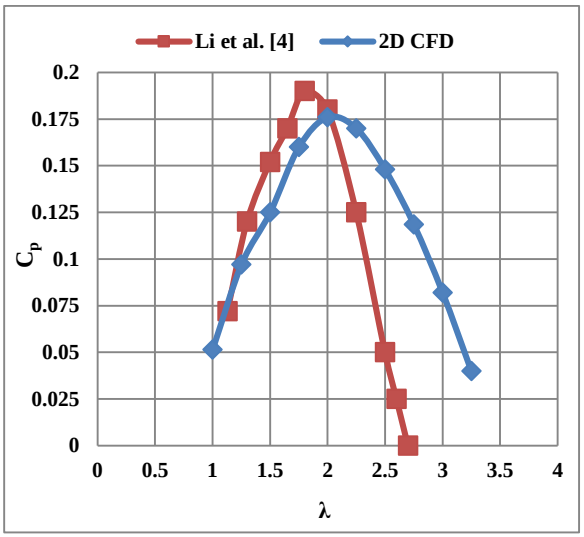

Figure 8. Validation of Cp

3.2. Effect Of Turbine Solidity

Geometric properties of different wind turbine models were given in Table 2.

Table 2. Details of Turbine Models

Model Name	Number of Blades (N)	Chord Length (c)	Rotor Radius (R)	Turbine Solidity (σ)
M1	3	0,265 m	0,75 m	0,53
M2	3	0,265 m	1 m	0,3975
M3	3	0,265 m	1,25 m	0,318

Solidity of a wind turbine changes with 3 different parameters. In this study, blade number and blade chord lengths were kept constant, while the turbine radius changed. The number of meshes for all turbine models were roughly the same. This is because element sizes for all edges and domains were kept the same as M2 model. Blade subdomain and rotating zone for all turbine models have also same dimensions, which includes majority of meshes. Solidity effect to the wind turbine aerodynamic characteristic is shown in Fig. 9.

When Figure 9 examined carefully, the highest Cp value observed for M2 was 0.176 in $\lambda = 2$ and the highest Cp value observed for M3 was 0.175 in $\lambda = 2.25$. When $\lambda = 3.25$, Cp value for M2 is 0.04 and Cp value for M3 is 0.09. In case of $\lambda = 1.25$, the observed Cp value for M2 is approximately 0.1, while the observed Cp value of M3 at the same TSR value is approximately 0.06. Maximum Cp value detected with M3 wind turbine model is approximately 0.57% lower than M2.

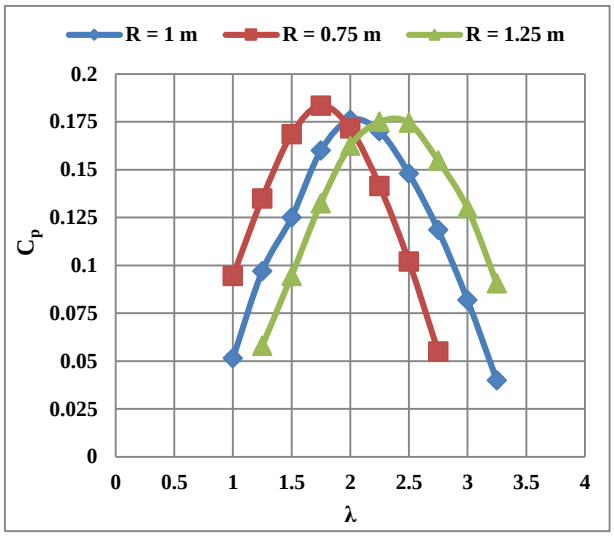

Figure 9. Power coefficient versus TSR as a function of Solidity

The highest Cp value observed for M1 was 0.1835 at $\lambda = 1.75$. For $\lambda = 1$, in the model with the same solidity, the Cp value is 0,095 and the Cp value observed for M2 is 0.05. In the case of $\lambda = 2.75$, the Cp value observed in the M1 turbine is 0.055, while the Cp value for M2 at the same λ value is 0.1185. Maximum Cp value detected with M1 wind turbine model is 4.25% higher than M2. The main reason for this situation is that the M1 blades move at a higher angular velocity than the other models at the same tsr value. When the results are examined, increasing rotor radius rises Cp at higher TSR values and reduces Cp at lower tsr values. Also, decreasing rotor radius increases Cp at lower tsr values and reduces Cp at higher TSR values.

Figure 10 shows the Cp values that vary according to the blade azimuth angles at different TSR values. When the Figure 10 is examined, a total of 3 peak points is seen in each round of the turbine. Maximum Cp values were observed at angles $\theta = 90, 210, 330°$ where turbine blades directly faced with the wind. It was seen that the maximum and minimum Cp values increase with increasing solidity in the range of $\lambda = 1.25$ and 1.75 in all 3 turbine models. In higher TSR values, the increase in solidity reduced the observed maximum and minimum Cp values. At points where the Cp value is below 0, the turbine does not have a self-start capability [10]. With the decrease of solidity, the maximum and minimum Cp values observed in the range of $\lambda = 1.25$ and 1.75 decreased, while in higher TSR values the maximum Cp value observed and the self-start ability of the wind turbine increased.

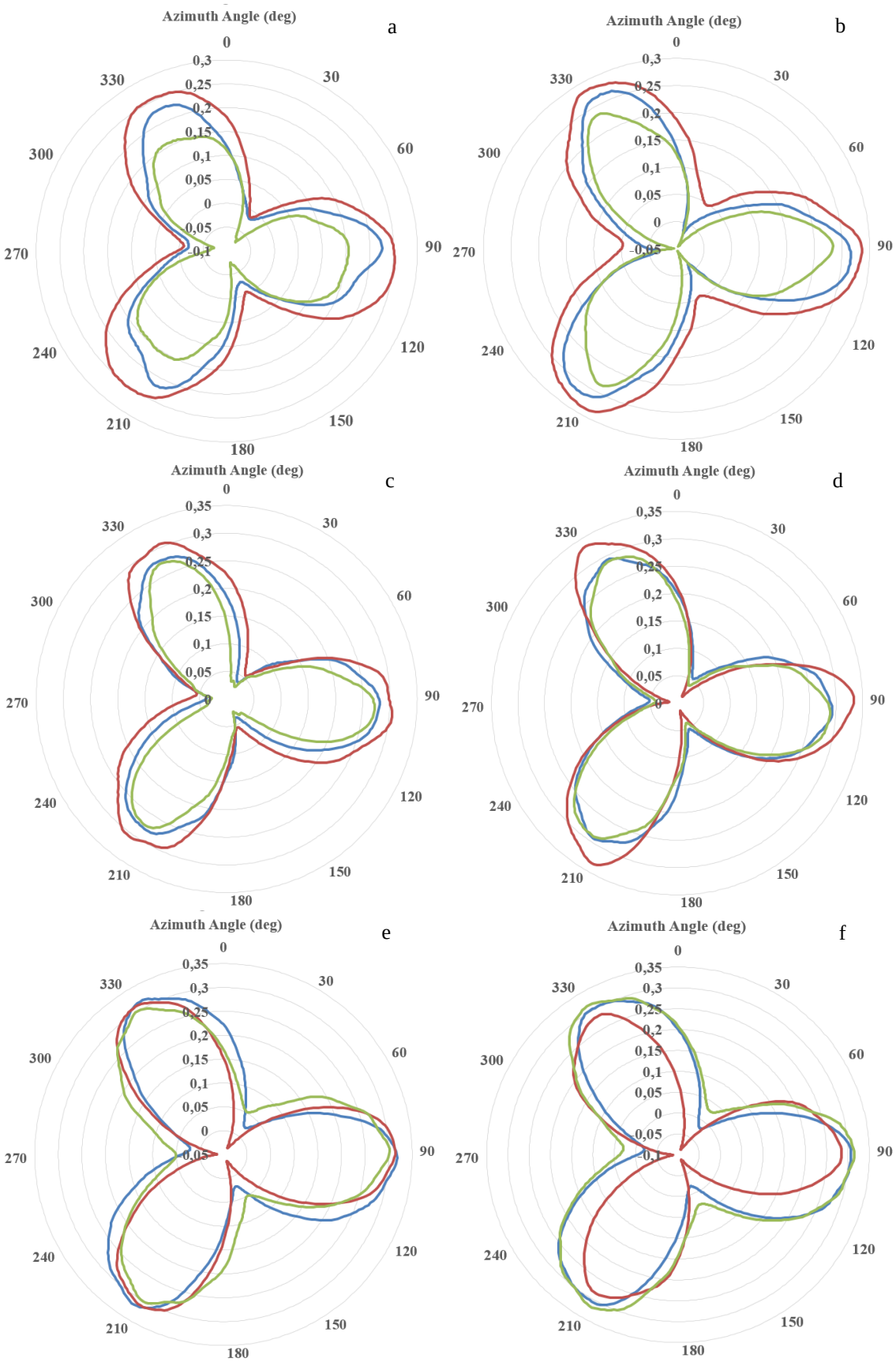

Figure 10. Averaged Power Coefficient against θ, for different TSR values (a) λ = 1,25 (b) λ = 1,5 (c) λ = 1,75 (d) λ = 2 (e) λ = 2,25 (f) λ = 2,5 (— Cp_M1 — Cp_M2 — Cp_M3)

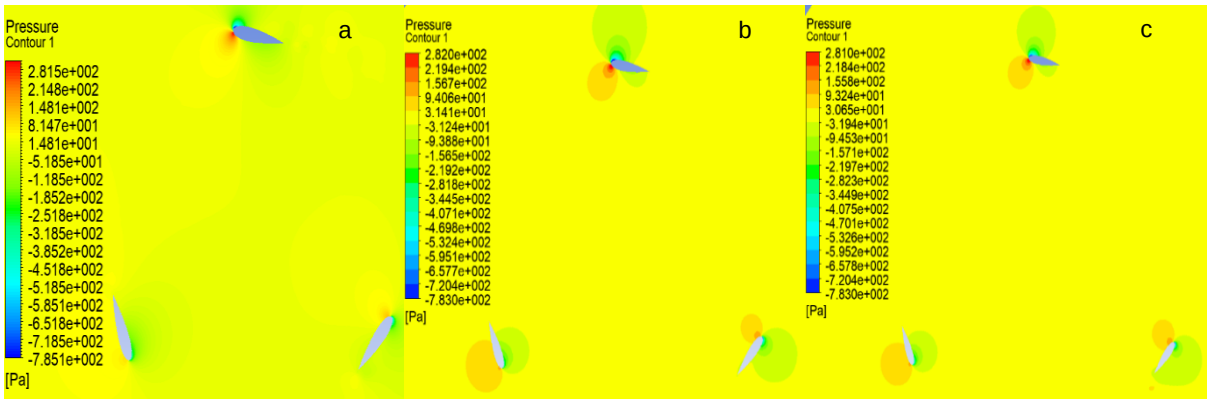

Figure 11. Pressure Contours (Pa) operating at λ = 2 (a) M1 (b) M2 (c) M3

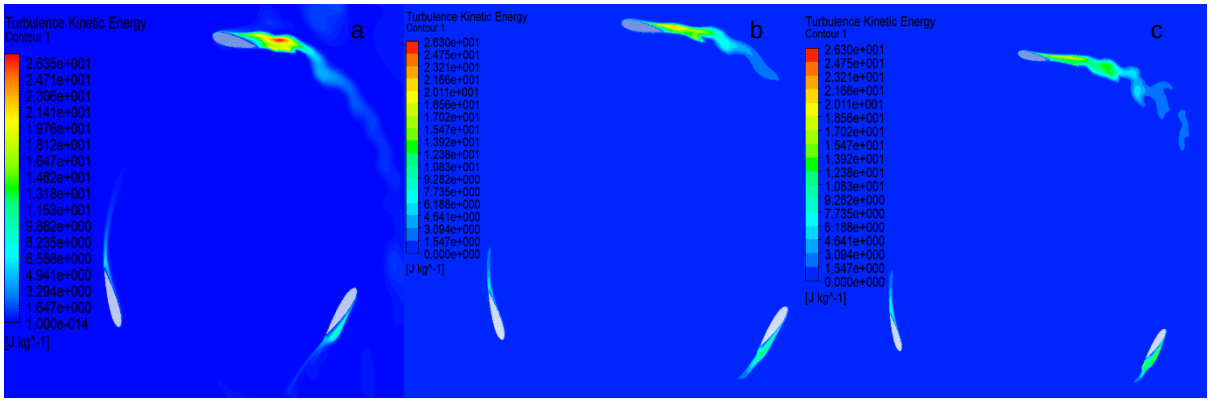

Figure 12. Turbulence Kinetic Energy contours operating at λ = 2 (a) M1 (b) M2 (c) M3

In Figures 11 and 12, the pressure and turbulence kinetic energy contours around the turbine models at different solidity values for λ = 2 are shown. When Figure 11 is examined, it is observed that the highest pressure affecting the blades when the maximum Cp value for λ = 2 (0.176) in the M2 turbine model. The lowest pressure affecting the blades in the same TSR value when the minimum Cp value (0.1625) in the M3 turbine model. Turbulent kinetic energy is defined as the energy that the vortex effect has, depending on the velocity of the flow in turbulent flow. As can be seen in Figure 12, increased turbulence kinetic energy has been observed due to the increase in solidity, because of the vortex structures on the blade surface.

In Figures 13 and 14, the pressure and turbulent kinetic energy contours that occur in a 360° round of a single blade in the turbine at different solidity and azimuth angles for λ = 2 are shown. As seen in Figure 13, the highest pressure value affecting the blades for all σ values was calculated when θ = 0°. With the increase in the angle of azimuth between 0° ≤ θ ≤ 180°, the pressure around the blades gradually decreased, while in the angle of azimuth between 180° ≤ θ ≤ 360°, the pressure gradually increased with the rise of the azimuth angle. In Figure 14, it can be seen that with the increase of solidity, high turbulence density is observed in the trailing edge region of the blades at both θ = 0° and 300° azimuth angles.

In general, it is observed that the M1 blade has a higher turbulence density than the other two turbine models as show in Fig. 12. The highest turbulence kinetic energy between 3 wind turbine models are occurred at θ = 0° due to pitch. As mentioned in the study, since the pitch angle is determined as 8°, when θ = 0° high pressure difference occurs between top and bottom surfaces of the blade. This happens because θ is close to the stall angle since it contains a low Reynolds number depending on wind speed. At the same time, turbulence kinetic energy has been observed to be more intense in areas with flow separation. These results are similar to other studies in the literature [38].

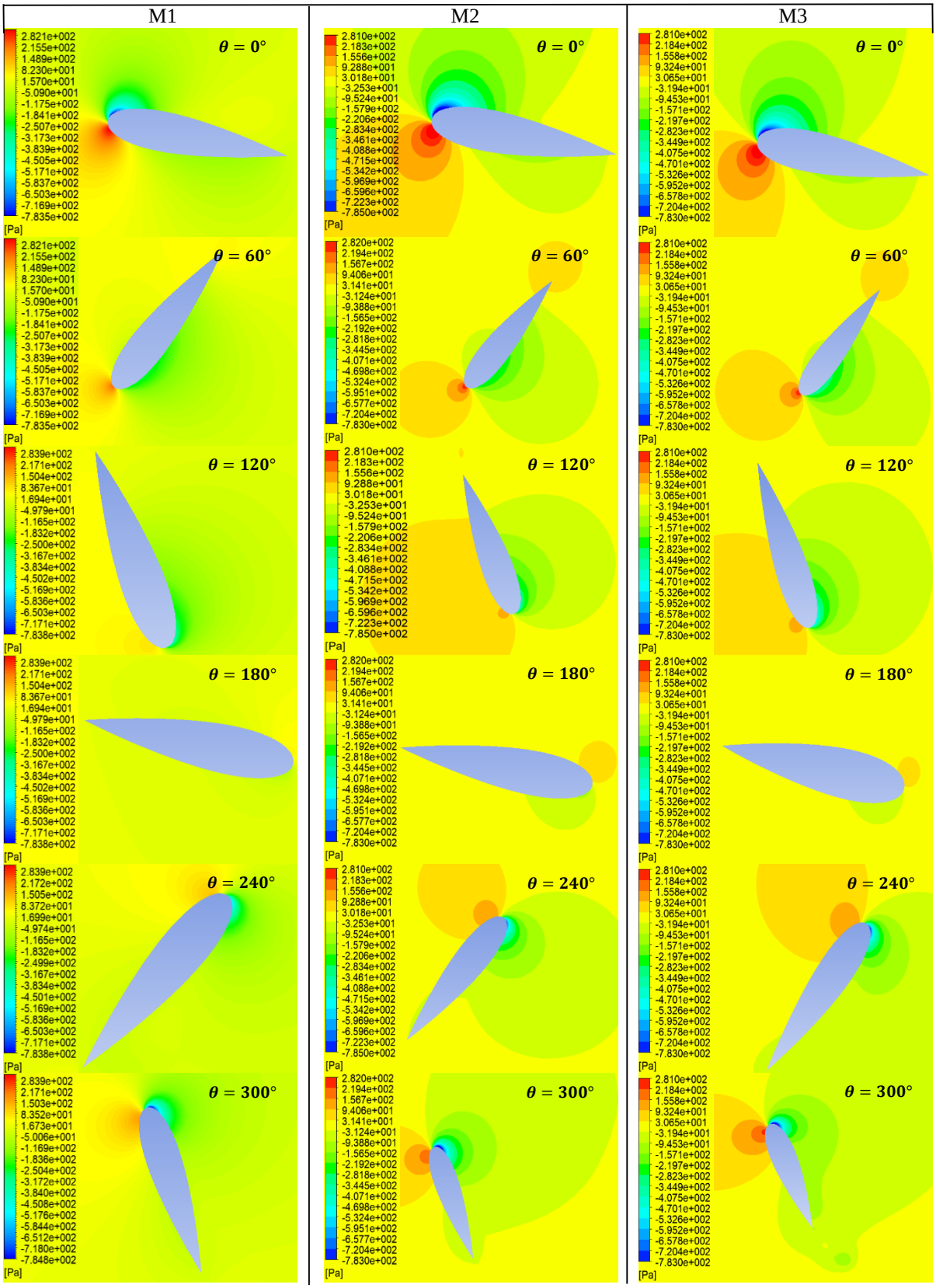

Figure 13. Pressure Contours around one blade for different σ, at various angular positions (See Table 2)

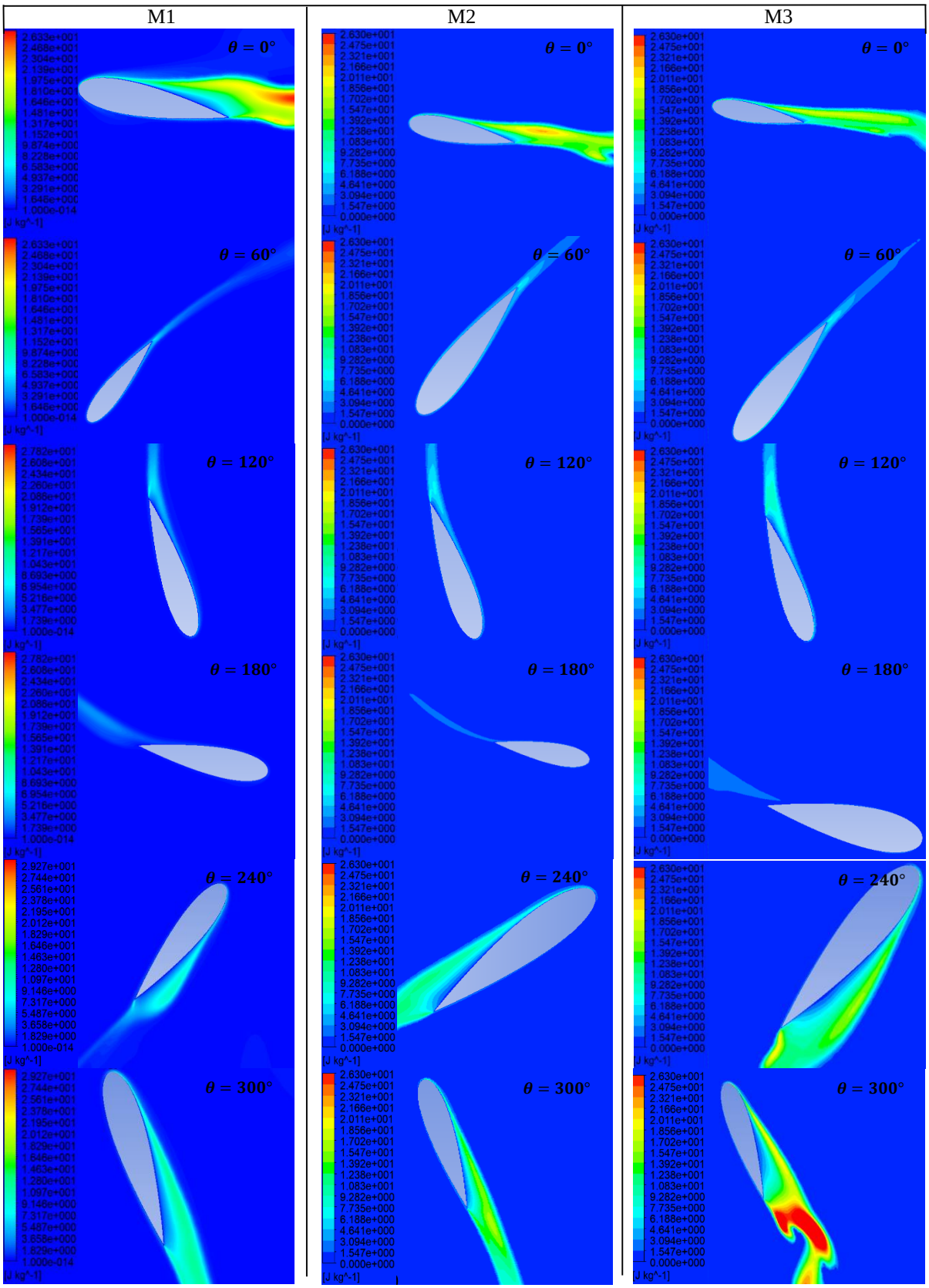

Figure 14. Turbulence kinetic energy contours around one blade for different σ, at various angular positions (See Table 2)

4. SUMMARY AND CONCLUSION

In this study, radius-dependent solidity effect to the aerodynamic characteristic of a H-rotor wind turbine has been modelled and numerically analysed with ANSYS Fluent 14.1 software in 2D. Findings obtained from this study are;

- To achieve independence from the mesh, 15 different mesh numbers were used and analyses were continued at 523611 mesh number.
- The maximum Cp values observed with M1, M2 and M3 turbine models are 0.1835, 0.176, 0.175, respectively.
- The Cp values of the M1, M3 wind turbine model according to M2 wind turbine model are increased by 4.25% and decreased by 0.57%, respectively.
- The wind turbine with a higher solidity has more coefficient of power in lower Tsr values.
- With the decrease of solidity, more coefficient of power can be observed in higher Tsr values.
- The increase of solidity increased the energy of the turbulent flow around the blades, and the decrease of solidity reduced the turbulence energy

NOMENCLATURE

A	swept area
C	blade chord length
C_D	drag coefficient
C_L	lift coefficient
C_m	moment coefficient
C_p	power coefficient
D	turbine diameter
F_L	lift force
F_D	drag force
G	generation of turbulence kinetic energy
H	rotor height
k	turbulence kinetic energy
N	number of blades
P	output power
R	rotor radius
T	time
T	output torque
U	wind speed
U_r	relative velocity
α	angle of attack
β	blade pitch angle
ε	turbulence dissipation rate
θ	azimuth angle
λ	tip speed ratio
μ	dynamic viscosity
μ_t	eddy viscosity
ρ	density
σ	rotor solidity
ω	angular velocity

DECLARATION OF ETHICAL STANDARDS

The author(s) of this article declare that the materials and methods used in this study do not require ethical committee permission and/or legal-special permission.

AUTHORS' CONTRIBUTIONS

Ahmet Fatih KAYA: Performed the experiments and analyse the results. Wrote the manuscript.

Himmet Erdi TANÜRÜN: Performed the experiments and analyse the results.

Adem ACIR: Analyse the results. Supervision.

CONFLICT OF INTEREST

There is no conflict of interest in this study.

REFERENCES

[1] Naccache G. and Paraschivoiu M., "Parametric study of the dual vertical axis wind turbine using CFD", ***J Wind Eng Ind Aerodyn,*** 172:244–55, (2018).

[2] Kragten A., "The Darrieus Rotor, A Vertical Axis Wind Turbine (VAWT) with Only A Few Advantages and Many Disadvantages", Sint-Oedenrode, (2004).

[3] Wong KH., Chong WT., Poh SC., Shiah YC., Sukiman NL. and Wang CT., "3D CFD simulation and parametric study of a flat plate deflector for vertical axis wind turbine", ***Renew Energy,*** 129:32–55, (2018).

[4] Li Q., Maeda T., Kamada Y., Murata J., Furukawa K. and Yamamoto M., "Effect of number of blades on aerodynamic forces on a straight-bladed Vertical Axis Wind Turbine", ***Energy,*** 90:784–95, (2015).

[5] Rezaeiha A., Montazeri H. and Blocken B., "Towards optimal aerodynamic design of vertical axis wind turbines: Impact of solidity and number of blades", ***Energy,*** 165:1129–48, (2018).

[6] Abu-el-yazied TG., Ali AM., Al-ajmi MS. and Hassan IM., "Effect of Number of Blades and Blade Chord Length on the Performance of Darrieus Wind Turbine", ***Am J Mech Eng,*** 2:16–25, (Autom 2015).

[7] Sunyoto A., Wenehenubun F., Sutanto H., "The effect of number of blades on the performance of H-Darrieus type wind turbine", International Conference on QiR, 192–6, (2013).

[8] Castelli MR., Betta S. De., Benini E., "Effect of Blade Number on a Straight-Bladed Vertical-Axis Darreius Wind Turbine", ***World Acad Sci Eng Technol,*** 6:256–62, (2012).

[9] Yang Y., Guo Z., Song Q., Zhang Y., Li Q., "Effect of blade pitch angle on the aerodynamic characteristics of a straight-bladed vertical axis wind

turbine based on experiments and simulations", ***Energies***, 11, (2018).

[10] Zhang LX., Liang Y. Bin., Liu. XH., Guo J., "Effect of blade pitch angle on aerodynamic performance of straight-bladed vertical axis wind turbine", ***J Cent South Univ,*** 21:1417–27, (2014).

[11] Fiedler AJ. and Tullis S., "Blade offset and pitch effects on a high solidity vertical axis wind turbine", ***Wind Eng***, 33:237–46, (2009).

[12] Bogateanu R., Dumitrache A., Dumitrescu H., Stoica CI., "Reynolds number efects on the aerodynamic performance of small VAWTs", ***UPB Sci Bull Ser D Mech Eng,*** 76:25–36, (2014).

[13] Gosselin R., Dumas G. and Boudreau M., "Parametric study of H-Darrieus vertical-axis turbines using CFD simulations", ***J Renew Sustain Energy***, 8, (2016).

[14] Bachant P. and Wosnik M., "Effects of reynolds number on the energy conversion and near-wake dynamics of a high solidity vertical-axis cross-flow turbine", ***Energies,*** 9:1–18, (2016).

[15] Li Q., Maeda T., Kamada Y., Murata J., Yamamoto M., Ogasawara T. et al., "Study on power performance for straight-bladed vertical axis wind turbine by field and wind tunnel test", ***Renew Energy***, 90:291–300, (2016).

[16] Siddiqui MS., Rasheed A., Kvamsdal T., Tabib M., "Effect of turbulence intensity on the performance of an offshore vertical axis wind turbine", ***Energy Procedia***, 80:312–20, (2015).

[17] Mălăel I., Drăgan V., Gherman B., "Turbulence intensity effects on the vertical axis wind turbine starting efficiency", ***Ann DAAAM Proc Int DAAAM Symp,*** 974–9, (2015-January).

[18] Ahmadi-Baloutaki M., Carriveau R., Ting DSK., "Performance of a vertical axis wind turbine in grid generated turbulence", ***Sustain Energy Technol Assessments***, 11:178–85, (2015).

[19] Carbó Molina A., De Troyer T., Massai T., Vergaerde A., Runacres MC., Bartoli G., "Effect of turbulence on the performance of VAWTs: An experimental study in two different wind tunnels", ***J Wind Eng Ind Aerodyn***, 193, (2019).

[20] Sobhani E., Ghaffari M., Maghrebi MJ., "Numerical investigation of dimple effects on darrieus vertical axis wind turbine", ***Energy***, 133:231–41, (2017) .

[21] Zamani M., Nazari S., Moshizi SA., Maghrebi MJ., "Three dimensional simulation of J-shaped Darrieus vertical axis wind turbine", ***Energy***, 116:1243–55, (2016) .

[22] Subramanian A., Yogesh SA., Sivanandan H., Giri A., Vasudevan M., Mugundhan V. et al., "Effect of airfoil and solidity on performance of small scale vertical axis wind turbine using three dimensional CFD model", ***Energy***, 133:179–90, (2017).

[23] Kumar R., Baredar P., "Solidity Study and its Effects on the Performance of A Small Scale Horizontal Axis Wind Turbine", ***Impending Power Demand Innov Energy Paths,*** 290–7, (2014).

[24] Liang C., Xi D., Zhang S., Yang Q., "Effects of Solidity on Aerodynamic Performance of H-Type Vertical Axis Wind Turbine", ***IOP Conference Series: Earth and Environmental Science,*** 170. 042061, (2018).

[25] G.J.M Darrieus., "Turbine having its rotating shaft transverse to the flow of the current" ***US Patent*** no. 1.835.018, (1931).

[26] Marsh P., Ranmuthugala D., Penesis I., Thomas G., "The influence of turbulence model and two and three-dimensional domain selection on the simulated performance characteristics of vertical axis tidal turbines", ***Renew Energy,*** 105:106–16, (2017).

[27] Şahin İ., Acir A., "Numerical and Experimental Investigations of Lift and Drag Performances of NACA 0015 Wind Turbine Airfoil", ***Int J Mater Mech Manuf***, 3:22–5, (2015).

[28] Alqurashi F., Mohamed MH., "Aerodynamic forces affecting the H-rotor darrieus wind turbine", ***Model Simul Eng,*** (2020).

[29] Danao LA., Qin N., Howell R., "A numerical study of blade thickness and camber effects on vertical axis wind turbines", ***Proc Inst Mech Eng Part A J Power Energy***, 226:867–81, (2012).

[30] Ferziger JH., Perić M., "Computational Methods for Fluid Dynamics", ***Berlin: springer,*** (2002).

[31] Mohamed MH., "Performance investigation of H-rotor Darrieus turbine with new airfoil shapes", ***Energy,*** 47:522–30, (2012).

[32] Roy S., Saha UK., "Computational study to assess the influence of overlap ratio on static torque characteristics of a vertical axis wind turbine", ***Procedia Eng***, 51:694–702, (2013).

[33] Tanürün HE., Acır A., "Modifiye Edilmiş NACA-0015 Kanat Yapısında Tüberkül Etkisinin Sayısal Analizi", ***J Polytech,*** 0900:185–95, (2019).

[34] Hashem I., Mohamed MH., "Aerodynamic performance enhancements of H-rotor Darrieus wind turbine", ***vol. 142. Elsevier B.V***, (2018).

[35] Roy S., Saha U., "Comparative analysis of turbulence models for flow simulation around a vertical axis wind turbine", ***Proceedings of Indo-Danish International Conference on WEMEP*** 22–23, (2012).

[36] Mohamed MH., Ali AM., Hafiz AA., "CFD analysis for H-rotor Darrieus turbine as a low speed wind energy converter", ***Engineering Science and***

Technology, an International Journal, 18:1-13, (2015).

[37] Sumantraa RB., Chandramouli S., Premsai TP., Prithviraj P., Vivek M., Kishore VR., "Numerical analysis of effect of pitch angle on a small scale vertical axis wind turbine", ***Int J Renew Energy Res***, 4:929–35, (2014).

[38] Tanürün HE., Ata İ., Canlı ME., Acır A., "Farklı Açıklık Oranlarındaki NACA-0018 Rüzgâr Türbini Kanat Modeli Performansının Sayısal ve Deneysel İncelenmesi", ***J Polytech***, 0900:371–381, (2020).